Theor Chem Acc (2012) 131:1126
DOI 10.1007/s00214-012-1126-x

REGULAR ARTICLE

Ab initio classical trajectory calculations of 1,3-cyclobutanedione radical cation dissociation

Jia Zhou · H. Bernhard Schlegel

Received: 1 March 2011 / Accepted: 11 August 2011 / Published online: 14 February 2012

Abstract The dissociation of 1,3-cyclobutanedione radical cation was studied by ab initio direct classical trajectory calculations at the BH&HLYP/6-31G(d) level of theory. A microcanonical ensemble using normal mode sampling was constructed by distributing 10 kcal/mol of excess energy above the transition state for the tautomerization of the keto-enol to the diketo form. A total of 210 trajectories were run starting from this transition state, yielding chemically activated 1, 3-cyclobutanedione radical cation. The majority of the trajectories resulted in $CH_2CO^{+\cdot} + CH_2CO$, with the activated CC bond breaking nearly twice as often as the spectator CC bond. The non-statistical behavior is observed because the rate of energy redistribution within the molecule is comparable to or slower than the dissociation rates. In addition to the expected products, dissociation to $CH_2COCH_2^{+\cdot} + CO$ and formation of a proton-transferred product $HCCO^{\cdot} + CH_3CO^{+}$ were also seen in some of the trajectories.

Keywords Cyclobutanedione · Ab initio MD · Branching ratio · Radical cation

1 Introduction

A chemically activated species can dissociate in a non-statistical manner if the rate for dissociation is faster than the rate for intramolecular energy redistribution. Acetone radical cation is an archetypal example of this process and has been studied experimentally and theoretically over the past 35 years [1–12]. Isomerization from the enol form to the keto form activates the newly formed methyl group that dissociates preferentially. Energy also flows to the other methyl group resulting in its dissociation at a slower rate and with a different energy distribution. The observed branching ratio is ca 1.5:1 in favor of the newly formed methyl group [1–9, 11, 12]. Similar to acetone radical cation, our ab initio MD study of pentane-2,4-dione radical cation [13] showed a competition between thermodynamics and non-statistical behavior in C–C bond dissociation. The activated terminal C–C bond had a lower dissociation probability than the weaker neighboring C–C bond. The two interior C–C bonds are equal in strength, but the one closer to the activated bond dissociates ca 20 times more frequently. Based on the above studies, it would be interesting to examine other chemically activated systems that would allow the flow of energy through several bonds of equal strength, thereby avoiding any thermodynamic bias. 1,3-Cyclobutanedione radical cation could be a good candidate. Upon isomerization to the diketo form, the energy from the activated C–C bond can flow sequentially to three other C–C bonds, potentially resulting in greater variety of non-statistical behavior than acetone radical cation. Experimentally, this reaction might be difficult to study because side reactions may compete with isomerization. However, in a theoretical study, the starting conditions can be chosen to avoid possible side reactions and focus on the competition between intramolecular energy flow and unimolecular dissociation (Scheme 1).

2 Method

Similar to our previous studies on acetone radical cation [11, 12] and pentanedione radical cation [13], we have used

Dedicated to Professor Vincenzo Barone and published as part of the special collection of articles celebrating his 60th birthday.

J. Zhou · H. B. Schlegel (✉)
Department of Chemistry, Wayne State University, Detroit, MI 48202, USA
e-mail: hbs@chem.wayne.edu

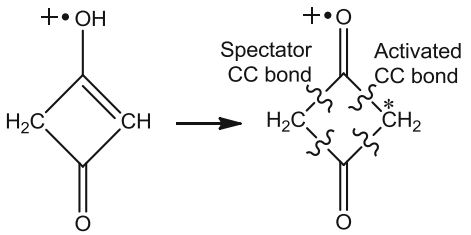

Scheme 1 Dissociation of 1,3-cyclobutanedione radical cation

ab initio classical trajectory calculations to study the non-statistical dissociation of 1,3-cyclobutanedione radical cation. The Gaussian suite of programs [14] was used for the ab initio electronic structure and molecular dynamics calculations. The geometries of the minima and transition states were optimized by Hartree–Fock (HF), hybrid density functional theory (B3LYP and BH&HLYP) [15–17] and second-order Møller–Plesset perturbation theory (MP2) [18]. Higher accuracy energy differences were calculated by the CBS-QB3 [19] and G4 [20] methods. The G4 calculations have a mean absolute deviation of 0.80 kcal/mol for 270 enthalpies of formation in the G3/05 test set and are used as a reference standard.

Ab initio classical trajectories were computed with BH&HLYP/6-31G(d) since this level of theory was in good agreement with the more accurate but more expensive methods. A Hessian-based predictor–corrector method [21, 22] was used to integrate the classical trajectories using a step size of 0.25 amu$^{1/2}$ bohr. The energy was conserved to better than 1×10^{-5} hartree, and the angular momentum was conserved to 1×10^{-8} ħ. Trajectories were initiated at the transition state for the keto-enol to diketo tautomerization. A microcannonical ensemble of initial states was constructed using normal mode sampling [23, 24]. As in our previous studies on acetone and pentanedione radical cations, a total energy of 10 kcal/mol above the zero point energy was added to the transition state. This initial energy was distributed among the 23 vibrational modes and translation along the transition vector toward the product. The total angular momentum was set to zero (corresponding to a rotationally cold distribution), and the phases of the vibrational modes were chosen randomly. The initial conditions are similar to those used previously for acetone radical cation [11, 12] and pentanedione radical cation [13]. A total of 210 trajectories were integrated starting from the transition state. Trajectories were terminated after 400 fs or when the centers of mass of the fragments were 8 bohr apart and the gradient between the fragments was less than 1×10^{-5} hartree/bohr.

3 Structures and energetics

The optimized geometries of the diketo and keto-enol forms of cyclobutanedione radical cation, various intermediates, transition states and products are shown in Fig. 1 for a number of levels of theory. The relative energies of these structures at the G4 level of theory are summarized in Fig. 2 and in Table 1. In its diketo form, 1,3-cyclobutanedione radical cation, **1**, has D_{2h} symmetry with a planar heavy-atom skeleton. The keto-enol form, **3**, also has a planar heavy-atom skeleton and lies 4.1 kcal/mol higher in energy than **1**. The keto-enol to diketo tautomerization of **3** via **TS2** to **1** produces a chemically activated cyclobutanedione radical cation. Breaking one CC bond has a barrier of only 6.6 kcal/mol and produces $CH_2C(O)CH_2CO^{+\cdot}$, **5**. Because of the release of ring strain, **5** is 14.6 kcal/mol more stable than **1**. Two CC dissociation paths lead from **5** to products with similar energies. One path yields $CH_2C(O)CH_2^{+\cdot}$ + CO, **6**, and requires 33.4 kcal/mol. The other path produces $CH_2CO^{+\cdot}$ + CH_2CO, **9**, via transition state **TS7** and intermediate **8** and has a barrier of 30.6 kcal/mol. The central CC bond in complex **8** is an odd electron bond and is very long (ca 2.4 Å). Nevertheless, it has a dissociation energy of 20.7 kcal/mol. Similar to our previous study on pentanedione radical cation [13], a proton transfer can occur between the products. This process happens via complex **10**, transition state **TS11** and complex **12**. The product CH_3CO^+ + $HCCO^{\cdot}$, **13**, is only 2 kcal/mol higher than **9**.

The relative energies of selected stationary points on the potential energy surface have been computed at a number of levels of theory and are compared in Table 1. Energies are calculated relative to $CH_2CO^{+\cdot}$ + CH_2CO, **9**, and the G4 relative energies are taken as reference values in the comparisons. As expected, the CBS-QB3 relative energies agree well with the G4 values, with mean average deviation (MAD) of 1.0 kcal/mol. Since the DFT methods were not able to locate structure **10**, QCISD geometries were used instead. The Hartree–Fock calculations greatly underestimate the stability of **1**, **TS2** and **8** relative to **9** and fail to locate structure **12**. The MP2 performs similar to B3LYP at predicting the relative energies (MAD of 3.7 and 3.6 kcal/mol, respectively) except that MP2 fails to locate the **TS4** structure. The BH&HLYP functional yields a lower MAD (1.9 kcal/mol), **TS2** is 3.5 kcal/mol too high, and **3** is 6.4 kcal/mol too stable, but the differences for the remaining structures are all less than 3 kcal/mol. Since the BH&HLYP calculations are in significantly better agreement with the G4 values than the HF, MP2 and B3LYP calculations, they have been used for the molecular dynamics simulations.

Fig. 1 Structures and selected geometric parameters of stationary points on the cyclobutanedione radical cation potential energy surface optimized at the BH&HLYP/6-31G(d) and G4 (B3LYP/6-31G(2df,p)) levels of theory (*top* and *bottom rows*, respectively). For structure **10**, QCISD/6-311G(d) value is listed. Bond distances are in angstroms. Relative energies in kcal/mol (given in parentheses) were calculated at the G4 level of theory ▶

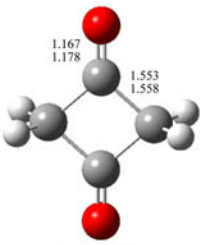

1, (-16.0)

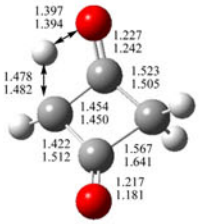

TS2, (56.8)

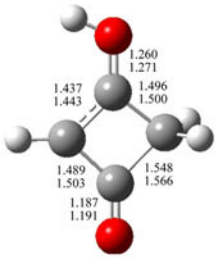

3, (-11.19)

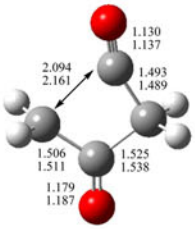

TS4, (-9.4)

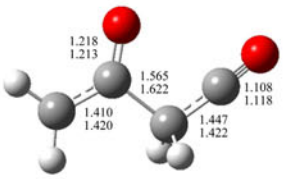

5, (-30.6)

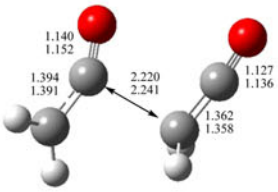

TS7, (-13.5)

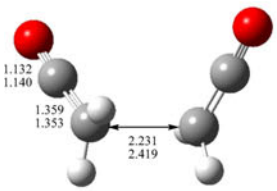

8, (-20.7)

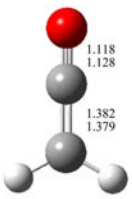

+

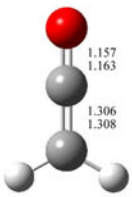

9, (0.0)

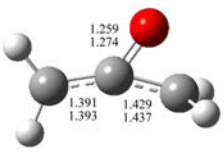

+

6, (2.8)

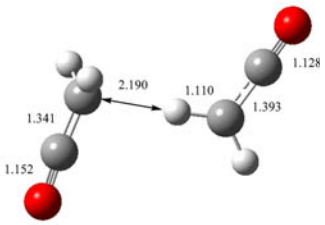

10, (-7.5)

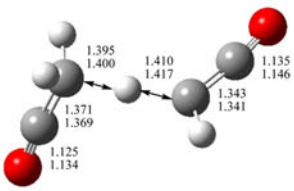

TS11, (-4.3)

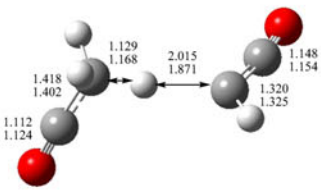

12, (-7.1)

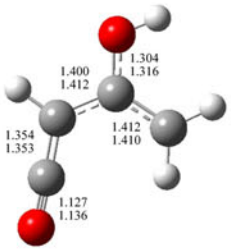

14, (-43.3)

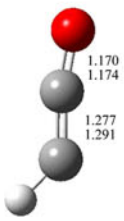

+

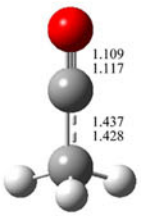

13, (1.9)

4 Dynamics

The trajectories were started at the keto-enol to diketo transition state **TS2** with initial conditions chosen from a microcanonical ensemble with 10 kcal/mol extra energy above the zero point energy of the transition state, and translation along the transition vector was directed toward the products. This modest amount of initial energy is somewhat arbitrary but assures that most of the trajectories reach the products in a timely fashion. Of the 210 trajectories that were integrated, seven had to be discarded because the energy was not conserved or the integration failed. Excluding these seven trajectories, the distribution of products is shown in Table 2. The keto-enol to diketo reaction produces cyclobutanedione radical cation with an activated CC bond. To be consistent with acetone radical cation, we designate the CC bond adjacent to the activated bond by a carbonyl group as the spectator CC bond. The activated CC bond, along with the CC bond opposite to it, dissociated in 93 trajectories producing $CH_2CO^{+\cdot} + CH_2CO$, **9**. The spectator CC bond and the CC bond opposite it dissociated in 50 trajectories. Four trajectories remained in the diketo minimum. There were 20 trajectories that did not reach the diketo minimum but crossed back to the keto-enol isomer; 15 of these trajectories ended with breaking of a CC bond to form $CH_2C(OH)CHCO^{+\cdot}$, **14**. Two trajectories yielded proton transfer products, **13**. Another two trajectories lost CO producing $CH_2COCH_2^{+\cdot} + CO$, **6** (one for each carbonyl group). Several trajectories stop after one CC bond breaking, yielding $CH_2COCH_2CO^{+\cdot}$, **5**. Of the four possibilities for breaking one CC bond, the activated CC bond broke most

Table 2 Branching ratios for cyclobutanedione radical cation dissociation from molecular dynamics at the BH&HLYP/6-31G(d) level of theory

Product structure	Description	Number of trajectories	Percentages
9	Active bond dissociation	93	45.8
9	Spectator bond dissociation	50	24.6
5	Active bond dissociation	17	8.4
5	Spectator bond dissociation	7	3.4
5	Opposite bond dissociation	8	4.0
6	CO elimination	2	1.0
13	Proton transfer	2	1.0
14	$CH_2C(OH)CHCO^{+\cdot}$	15	7.5
1	Cyclobutanedione radical cation	4	2.0
3	Enol isomer	5	2.5

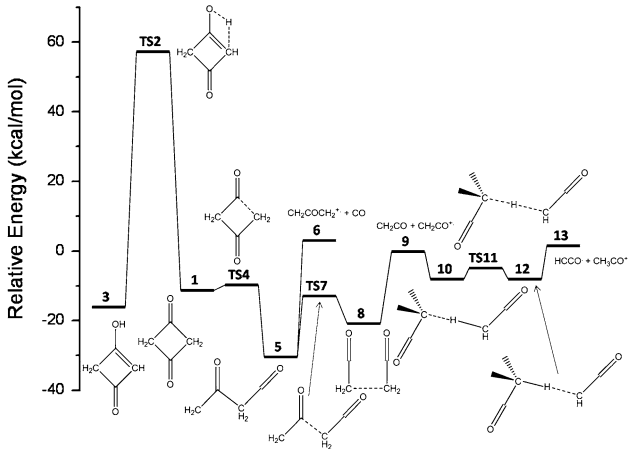

Fig. 2 Potential energy profile for the isomerization and dissociation of cyclobutanedione radical cation computed at the G4 level of theory

Table 1 Relative energies (kcal/mol) of various points on the cyclobutanedione radical cation potential energy surface

	HF/6-31G(d)	B3LYP/6-31G(d)	MP2/6-31G(d)	BH&HLYP/6-31G(d)	CBS-QB3	G4
1	7.8	−24.4	−21.3	−18.6	−20.0	−16.0
TS2	75.7	51.4	72.3	60.3	54.3	56.8
3	−10	−13.6	−3.5	−18.3	−12.6	−11.9
TS4	1.8	−11.9	−9.7[a]	−10.8	−8.3	−9.4
5	−31.9	−30	−28.3	−33.3	−30.2	−30.6
6	−1.9	4.1	−0.4	1.2	3.6	2.8
TS7	−4.4	−18.7	−18.2	−14.7	−12.1	−13.5
8	−6.0	−27.9	−25.9	−21.9	−21.5	−20.7
9	0.0	0.0	0.0	0.0	0.0	0.0
10	−4.1	−13.4[a]	−8.6	−8.4[a]	−6.5[b]	−7.5[b]
TS11	6.5	−11.1	−6.5	−5.2	−3.5	−4.3
12	[c]	−10.4	−8.6	−6.8	−6.4	−7.1
13	5.1	2.6	2.8	3.8	2.1	1.9
14	−36.9	−44.3	−42.2	−45.6	−43.2	−43.3
MAD	8.4	3.6	3.7	1.9	1.0	

[a] Single-point energy at QCISD/6-311G(d) geometry plus QCISD/6-311(d) ZPE

[b] Using QCISD/6-311G(d) geometry

[c] Stationary point could not be located

frequently (17 trajectories), followed by the spectator CC bond (seven trajectories) and the other two bonds (four trajectories each).

In acetone radical cation, the two CC bonds have equal bond energies and are expected to dissociate at equal rates. The observed branching ratio of ca 1.5–1 thus indicates significant non-statistical behavior. In pentanedione, the active versus spectator bond dissociation ratio is complicated by differences in the bond strengths. Nevertheless, comparison with RRKM (Rice–Ramsperger–Kassel–Marcus) rate calculations indicates significant non-statistical behavior. The situation is simpler for cyclobutanedione radical cation, since all of the CC bonds have the same dissociation energy. There are two ways to produce $CH_2CO^{+\cdot} + CH_2CO$, **9**, depending on whether the active CC bond or spectator CC bond breaks. Statistically, they would be expected to have the same dissociate rate, but the molecular dynamics calculations yield a ratio of $93{:}50 = 1.86$ for active versus spectator CC bond dissociation. This is a greater deviation from statistical behavior than for acetone radical cation with the same initial conditions. As in acetone radical cation, it is the result of competition between the rate of dissociation and the rate of intramolecular energy flow. In solution, collisions with the solvent may help redistribute the energy and thus reduce the non-statistical behavior. Thus, the non-statistical behavior should be greatest in the gas phase.

Acknowledgments This work was supported by a grant from the National Science Foundation (CHE0910858). Computer time made available by Computing Grid of Wayne State University is gratefully acknowledged.

References

1. Depke G, Lifshitz C, Schwarz H, Tzidony E (1981) Angew Chem Int Ed 20:792
2. McAdoo DJ, Hudson CE (1984) Int J Mass Spectrom Ion Processes 59:77
3. McAdoo DJ, McLafferty FW, Smith JS (1970) J Am Chem Soc 92:6343
4. Turecek F, Hanus V (1984) Organic Mass Spectrom 19:631
5. Heinrich N, Louage F, Lifshitz C, Schwarz H (1988) J Am Chem Soc 110:8183
6. Lifshitz C, Tzidony E (1981) Int J Mass Spectrom Ion Physics 39:181
7. Lifshitz C (1983) J Phys Chem 87:2304
8. Lifshitz C, Tzidony E, Terwilliger DT, Hudson CE (1980) Adv Mass Spectrom 8A:859
9. Osterheld TH, Brauman JI (1993) J Am Chem Soc 115:10311
10. Nummela JA, Carpenter BK (2002) J Am Chem Soc 124:8512
11. Anand S, Schlegel HB (2004) Phys Chem Chem Phys 6:5166
12. Zhou J, Schlegel HB (2008) J Phys Chem A 112:13121
13. Zhou J, Schlegel HB (2009) J Phys Chem A 113:1453
14. Frisch MJ, Trucks GW, Schlegel HB, Scuseria GE, Robb MA, Cheeseman JR, Montgomery JA Jr, Vreven T, Kudin KN, Burant JC, Millam JM, Iyengar SS, Tomasi J, Barone V, Mennucci B, Cossi M, Scalmani G, Rega N, Petersson GA, Nakatsuji H, Hada M, Ehara M, Toyota K, Fukuda R, Hasegawa J, Ishida M, Nakajima T, Honda Y, Kitao O, Nakai H, Klene M, Li X, Knox JE, Hratchian HP, Cross JB, Bakken V, Adamo C, Jaramillo J, Gomperts R, Stratmann RE, Yazyev O, Austin AJ, Cammi R, Pomelli C, Ochterski JW, Ayala PY, Morokuma K, Voth GA, Salvador P, Dannenberg JJ, Zakrzewski VG, Dapprich S, Daniels AD, Strain MC, Farkas O, Malick DK, Rabuck AD, Raghavachari K, Foresman JB, Ortiz JV, Cui Q, Baboul AG, Clifford S, Cioslowski J, Stefanov BB, Liu G, Liashenko A, Piskorz P, Komaromi I, Martin RL, Fox DJ, Keith T, Al-Laham MA, Peng CY, Nanayakkara A, Challacombe M, Gill PMW, Johnson B, Chen W, Wong MW, Gonzalez C, Pople JA (2007) Gaussian DV, revision F02. Gaussian Inc, Wallingford, CT, USA
15. Becke AD (1993) J Chem Phys 98:1372
16. Becke AD (1993) J Chem Phys 98:5648
17. Lee C, Yang W, Parr RD (1988) Phys Rev B 37:785
18. Moller C, Plesset MS (1934) Phys Rev 46:618
19. Montgomery JA, Ochterski JW, Peterson GA (1994) J Chem Phys 101:5900
20. Larry AC, Paul CR, Krishnan R (2007) J Chem Phys 126:084108
21. Bakken V, Millam JM, Schlegel HB (1999) J Chem Phys 111:8773
22. Millam JM, Bakken V, Chen W, Hase WL, Schlegel HB (1999) J Chem Phys 111:3800
23. Hase WL (1998) In: Schleyer PvR, Allinger NL, Clark T, Gasteiger J, Kollman PA, Schaefer III HF, Schreiner PR (eds) Encyclopedia of computational chemistry. Wiley, Chichester, p 402
24. Peslherbe GH, Wang H, Hase WL (1999) Adv Chem Phys 105:171